Supplementary material

Tailoring the composition of one-step electrodeposited Co,Ni/Co,Ni(OH)$_2$ composite coating for highly active hydrogen evolution electrode

Karolina Kordek, Ewa Lorenc-Grabowska and Piotr Rutkowski*

Department of Polymer and Carbonaceous Materials, Faculty of Chemistry,
Wrocław University of Science and Technology, Gdańska 7/9, 50-344 Wrocław, Poland

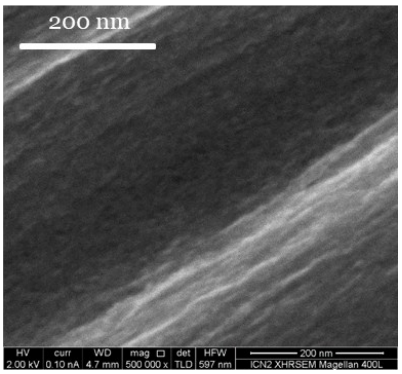

Figure S1 The SEM images for the hCT electrode.

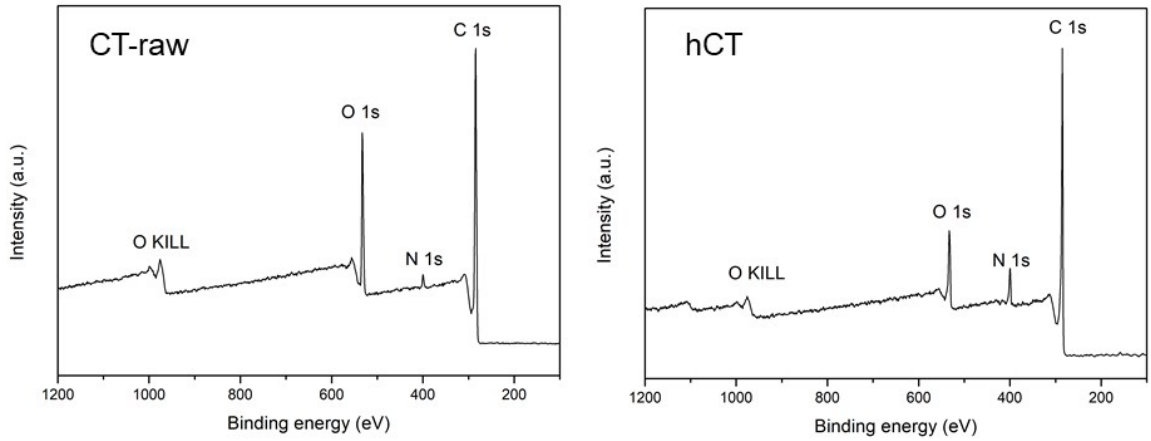

Figure S2 XPS survey spectrum of the CT-raw and hCT electrode.

Table S1 The atomic concentrations of elements in the surface of the CT-raw and hCT electrodes.

	at.%		
	C	O	N
CT-raw	78.9	19.0	2.13
hCT	80.8	10.4	8.86

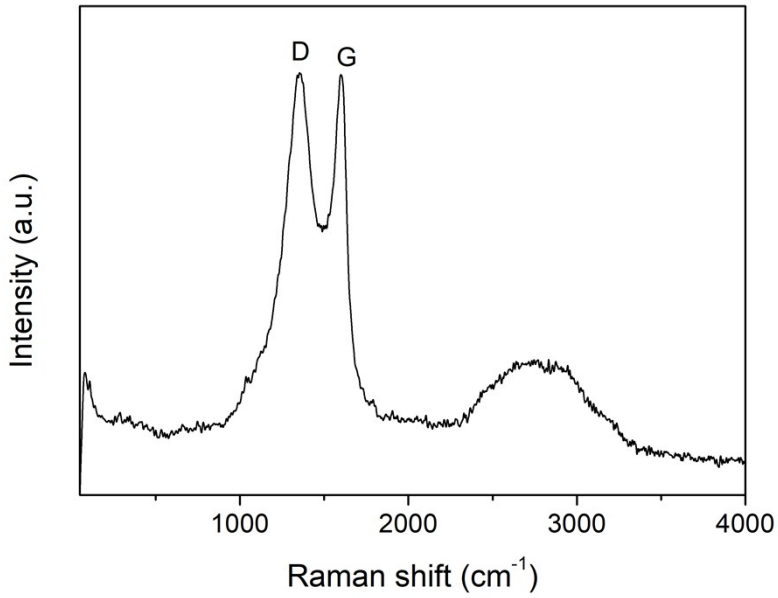

Figure S3 Raman spectrum of the hCT electrode.

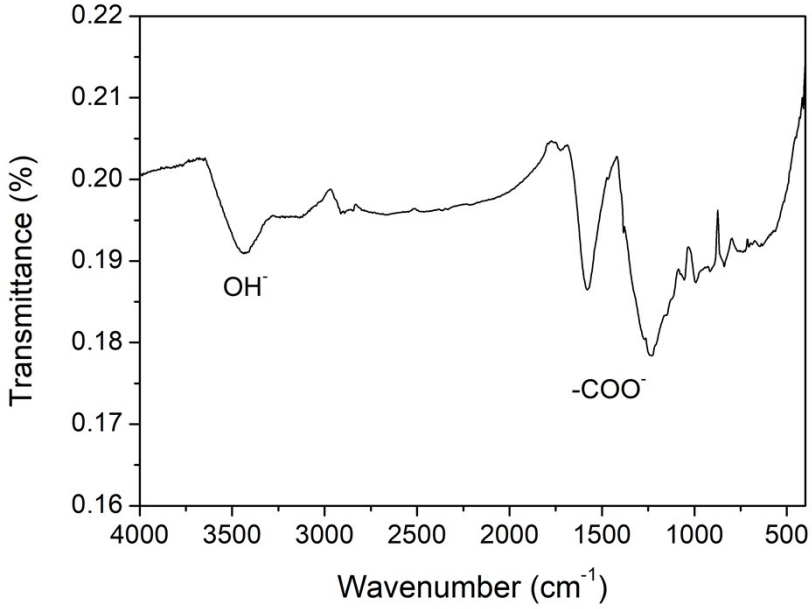

Figure S4 FT-IR spectrum of the hCT electrode.

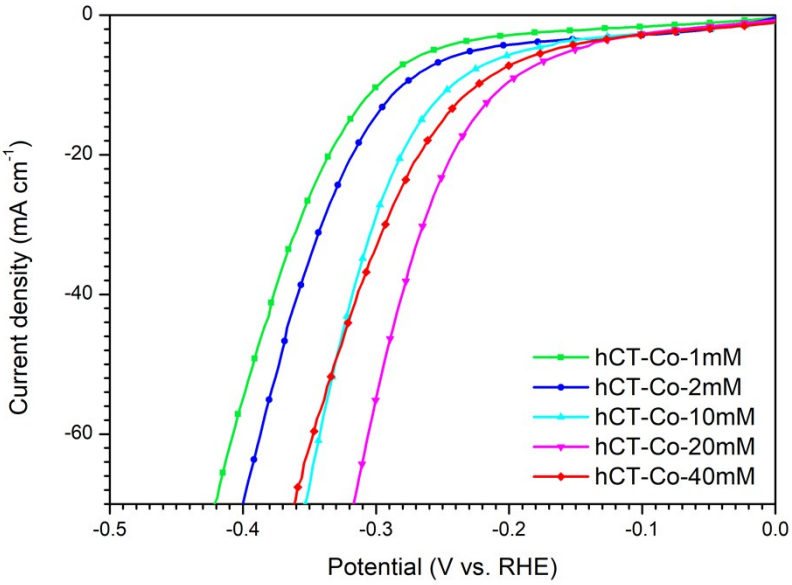

Figure S5 LSV plots for the series of electrodes with variable cobalt concentration in the solution for electrodeposition.

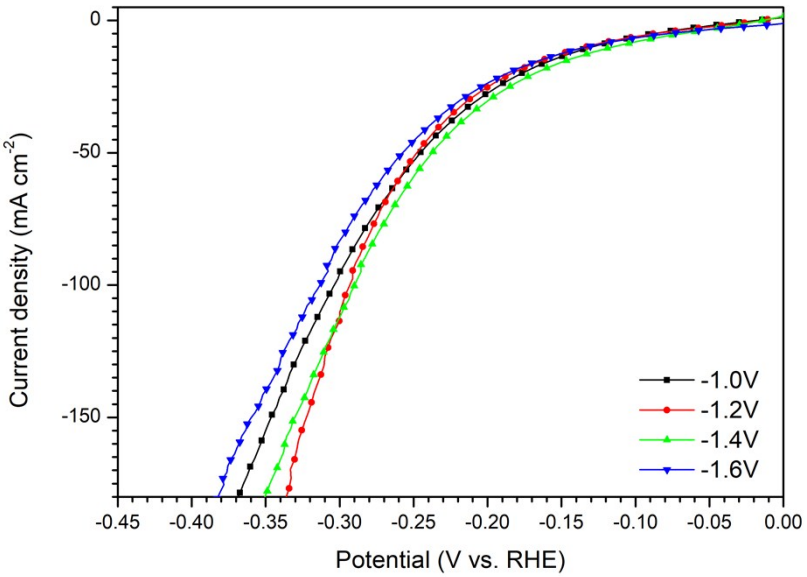

Figure S6 LSV plots for the series of electrodes with variable deposition potential.

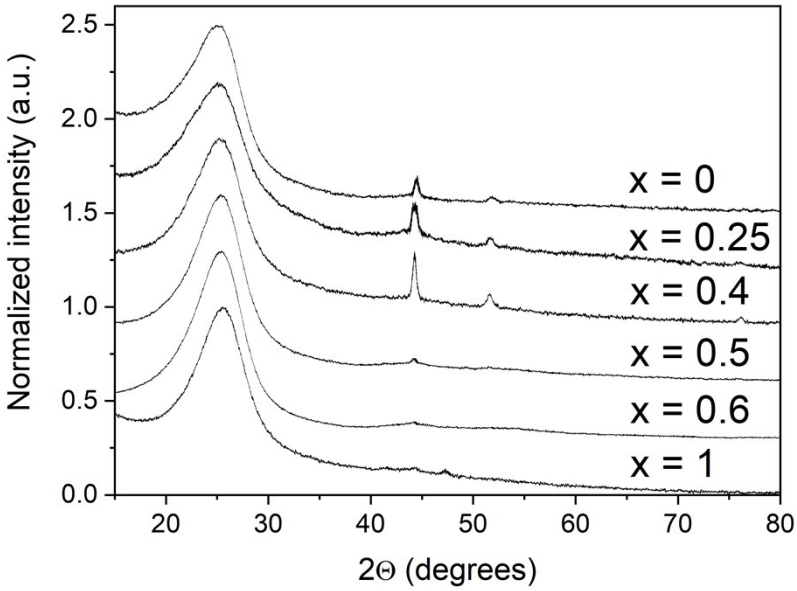

Figure S7 The wide angle XRD spectra for hCT-Co_xNi_{1-x} electrodes.

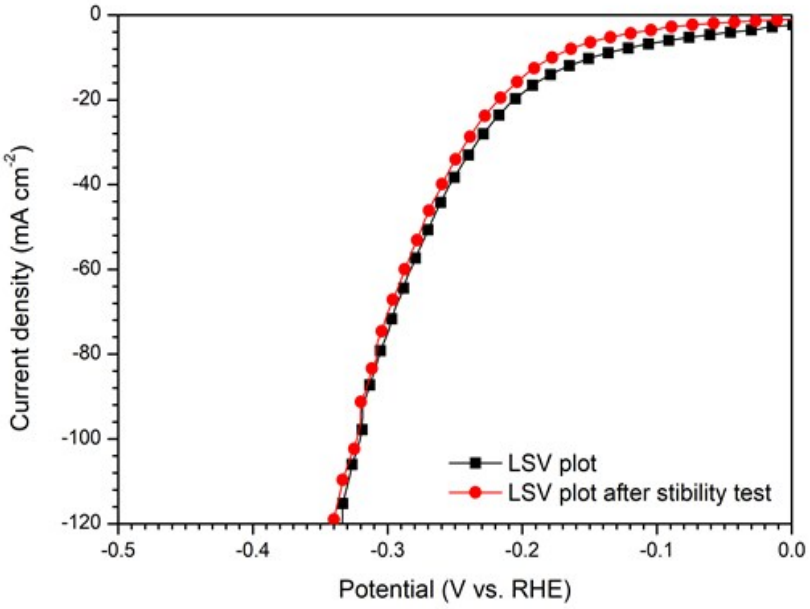

Figure S8 Comparison of LSV plots for hCT-$Co_{0.4}Ni_{0.6}$ before and after the stability test for 100 h at the current density of 10 mA cm^{-2}.

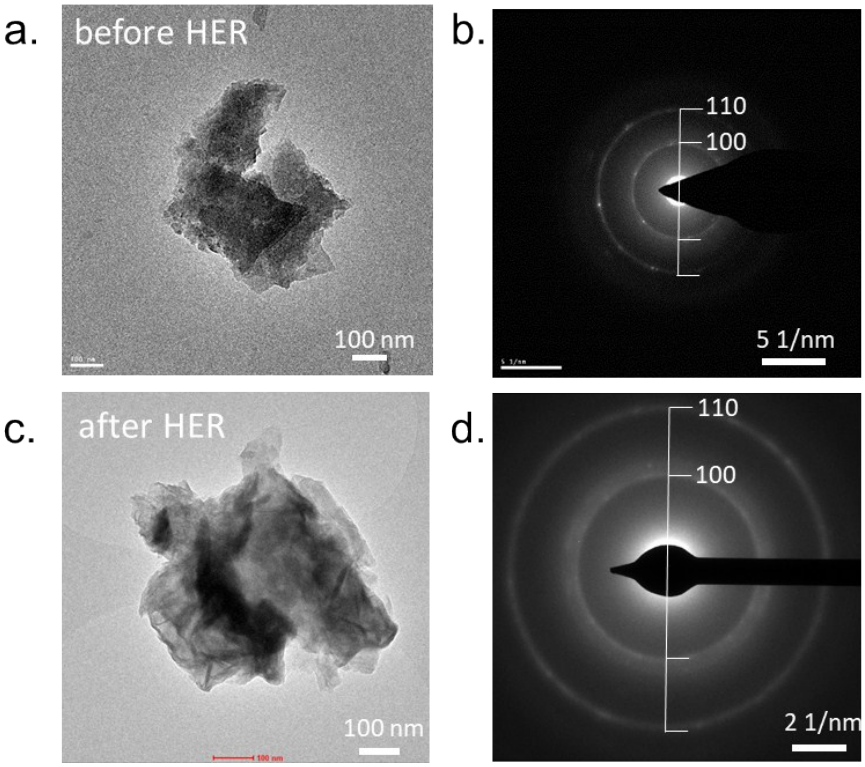

Figure S9 TEM images of hCT-$Co_{0.4}Ni_{0.6}$ electrode (a) before and (c) after the stability test and corresponding SAED patterns (b) before and (d) after the stability test.

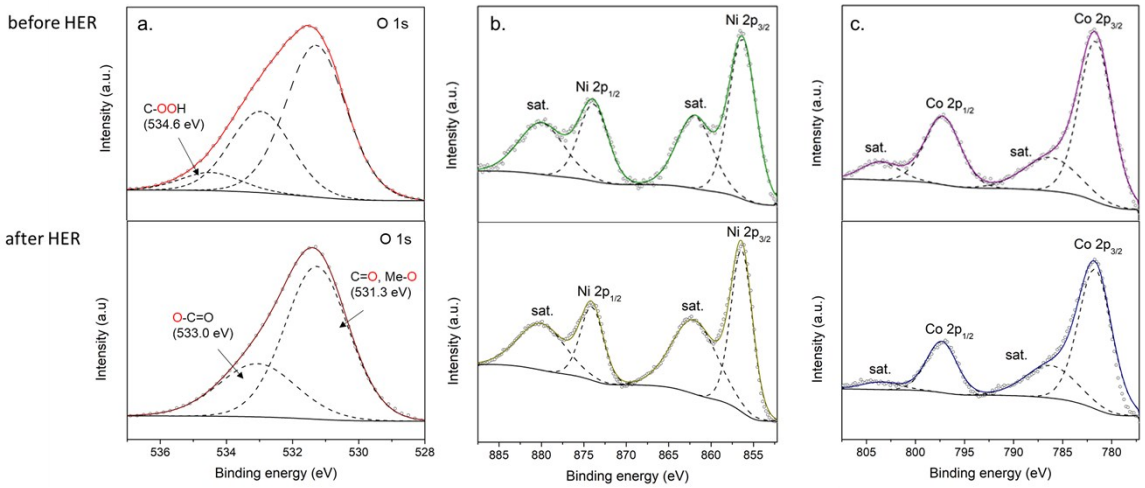

Figure S10 Comparison of high-resolution XPS spectra of hCT-$Co_{0.4}Ni_{0.6}$ electrode before and after the HER stability test in (a) O 1s, (b) Ni 2p and (c) Co 2p regions.

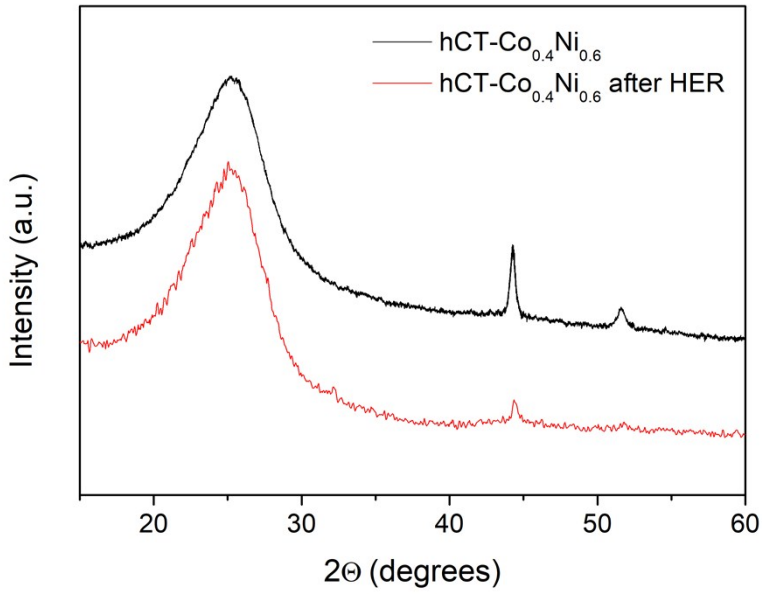

Figure S11 Comparison of XRD diffractograms of hCT-$Co_{0.4}Ni_{0.6}$ electrode before and after HER stability test.

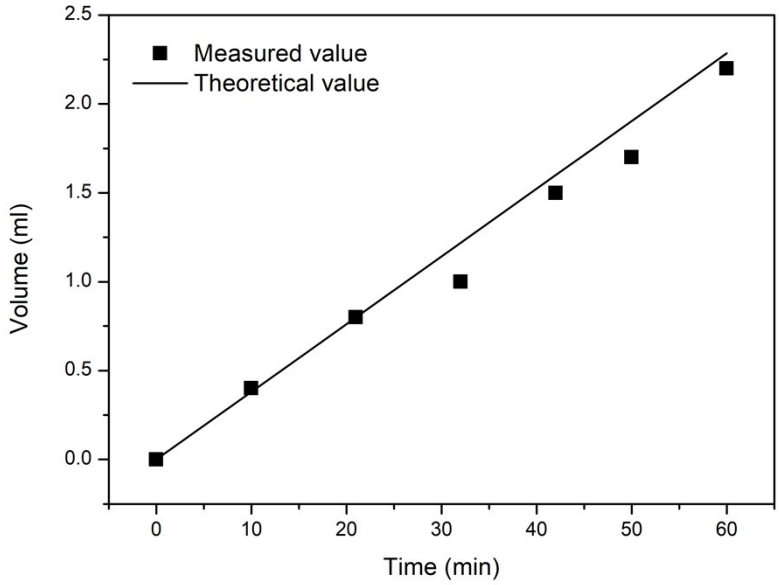

Figure S12 Experimental and theoretical volumes of H2 evolved from hCT-$Co_{0.4}Ni_{0.6}$ electrode at a potential of -0.1 V vs. RHE, measured for 60 min.

hCT-Ni

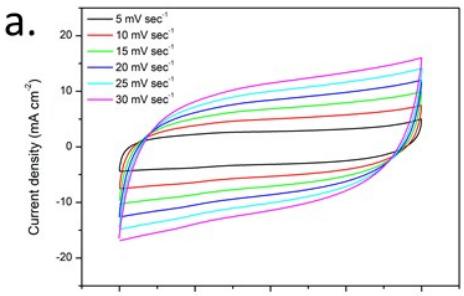

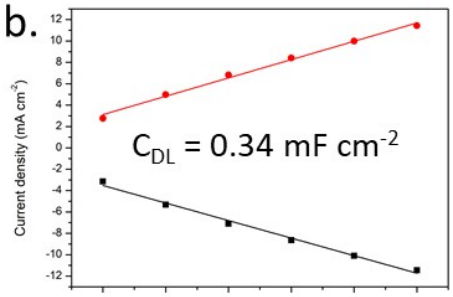

hCT-$Co_{0.25}Ni_{0.75}$

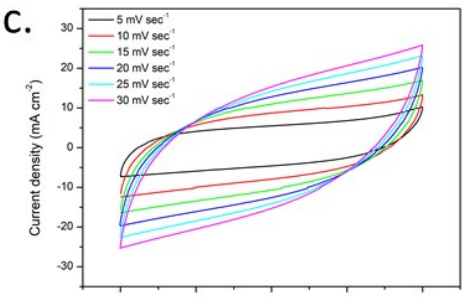

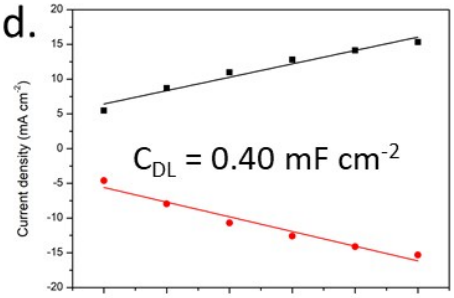

hCT-$Co_{0.4}Ni_{0.6}$

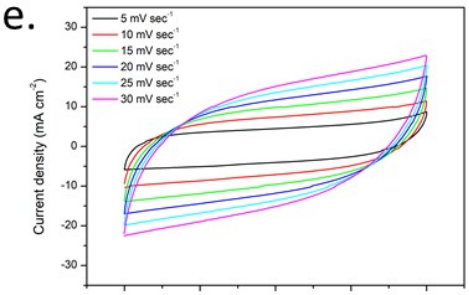

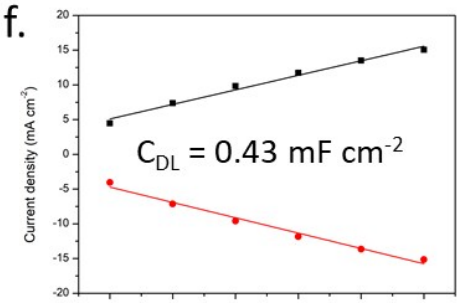

hCT-$Co_{0.5}Ni_{0.5}$

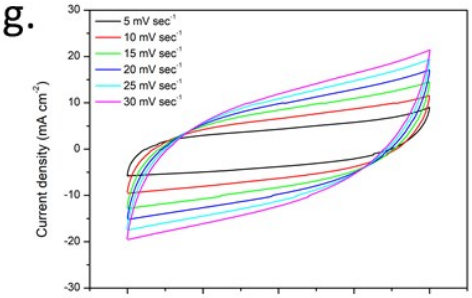

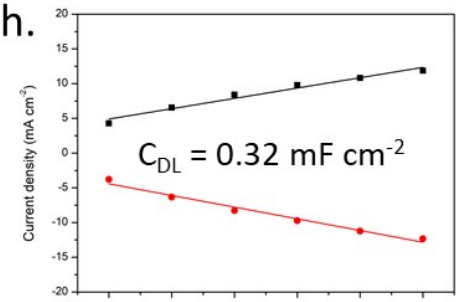

hCT-$Co_{0.6}Ni_{0.4}$

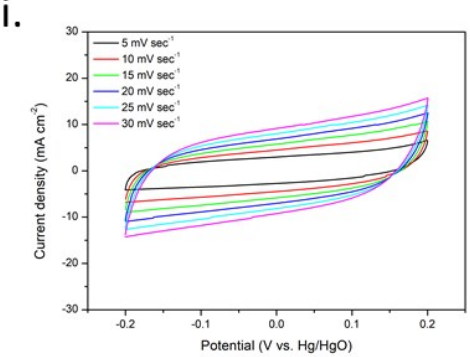

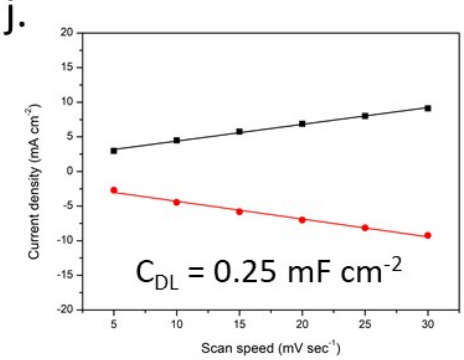

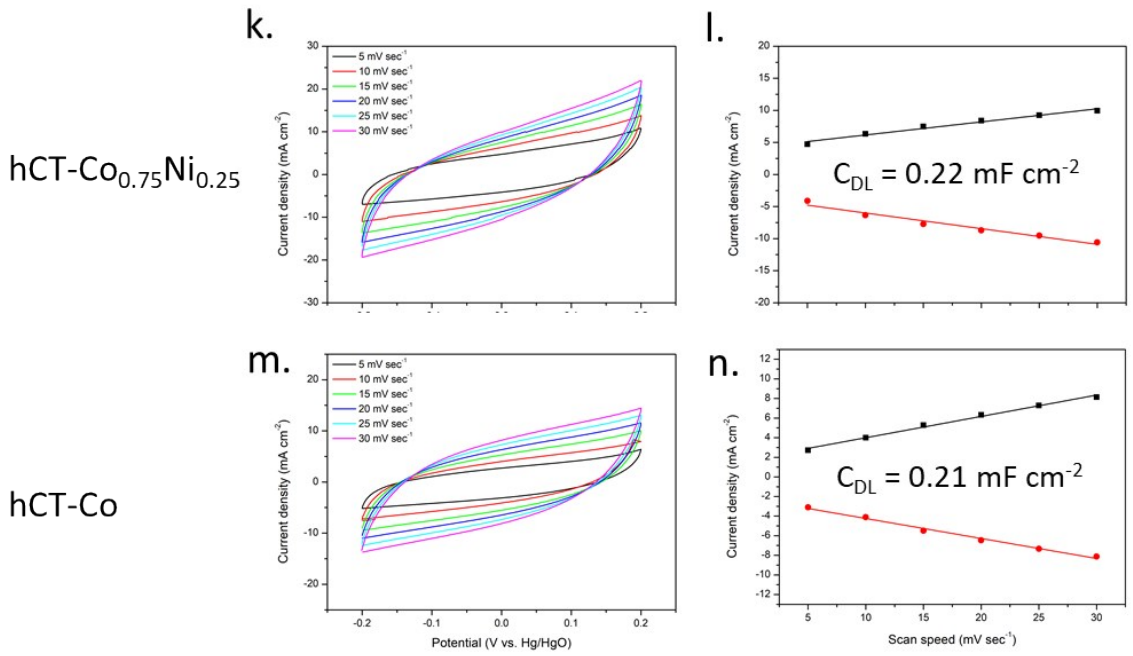

Figure S13 CV plots at different scan rates and corresponding linear fits of current densities versus scan speeds.

Table S2 Comparison of the HER overpotentials of the recently published noble metal-free electrocatalysts in 1.0 M KOH.

Material	Overpotential at 10 mA cm^{-2} [mV]	Reference
NiCoFe LTHs/CFC	200	A.L. Wang et. al, ACS Energy Lett., **2016**, 1, 445
CoFe LDH-F	255	P.F. Liu, ACS Appl. Mater. Interfaces, **2016**, 8 34474
Co-Fe	163	W. Liu et. al, Nano Energy, **2016**, 38, 576
δ-FeOOH NSs	108	B. Liu et. al., Adv. Mater, **2018**, 30, 1803144
Ni1.5Fe0.5P	282	H. Huang et. al, Nano Energy **2017**, 34, 472
Ni-Co-Ti	125	P. Ganesan et. al, ACS Appl. Mater. Interfaces, **2017**, 9 (14), 12416
NiS0.28O0.72	140	J. Liu et. al, Small **2017**, 13, 1602637
NiCo2S4 NW/NF	210	A. Sivanantham et al., Adv. Funct. Mater. **2016**, 26, 4661–4672.
CoFe/NF	110	P. Babar et. al, Small, **2018**, 14, 1702568
2D-MoS_2/$Co(OH)_2$	128	Z. Zhu et. al, Adv. Mater, **2018**, 30, 1801171
$NiCo_2O_4$/NiFe LDH	192	Z. Wang et. al, ACS Appl. Mater. Interfaces, **2017**, 9, 1488
$Ni_{12}P_5$	170	P.W. Menezes et. al, ACS Catal., **2017**, 7, 103
Cu/CoS_x	134	Y. Liu et. al, Adv. Mater, **2017**, 29, 1606200
Cu@NiFe LDH	116	L. Yu et. al, Energy Environ. Sci., **2017**, 8, 1820
cobalt/nickel-based films on CF	150	this work